To cite this article: ZHANG M, WANG J H, WAN D C. Multi-state luxury cruise ship seakeeping based on overlapping grids [J/OL]. Chinese Journal of Ship Research, 2022, 17(2). http://www. ship-research. com/en/article/doi/10.19693/j.issn.1673-3185.02277.

DOI: 10.19693/j.issn.1673-3185. 02277

Multi-state luxury cruise ship seakeeping based on overlapping grids

ZHANG Mu[1,2], *WANG Jianhua*[1,2], *WAN Decheng*[*1,2]

1 Computational Marine Hydrodynamics Laboratory, Shanghai Jiao Tong University, Shanghai 200240, China
2 School of Naval Architecture, Ocean and Civil Engineering, Shanghai Jiao Tong University, Shanghai 200240, China, Shanghai 200240, China

Abstract: [**Objective**] In the design stage of a luxury cruise ship, to save costs, it is necessary to use the computational fluid dynamics (CFD) method to predict the seakeeping performance of the cruise ship under design. [**Method**] The research object of this paper is a large luxury cruise ship. The self-developed ship hydrodynamic CFD solver naoe-FOAM-SJTU is used to simulate the seakeeping performance of the model-scale luxury cruise ship. The seakeeping simulation adopts the speed-inlet input wave-making method and predicts and summarizes the cruise ship motion under different wave heights and wave directions. [**Results**] The evaluation finds that the designed model-scale cruise ship basically meets the requirements of ship comfort under the maximum speed and wave heights of 0.062 5, 0.1, and 0.15 m, and it meets the requirements of ship safety under the designed speed, a wave height of 0.225 m, and head sea condition. [**Conclusion**] Under the calculated working conditions, this cruise ship type design conforms to the safety and comfort standards in the seakeeping performance evaluation standards for luxury cruise ships.

Key words: luxury cruise ship; overlapping grids; seakeeping performance evaluation; naoe-FOAM-SJTU

CLC number: U661.32; U661.33^{+}8

0 Introduction

Luxury cruise ship is regarded as the most dazzling pearl on the crown of the shipbuilding industry. It is a high-tech ship integrating high technology, high added value, and high reliability. In 2018, a government document titled *Some Opinions and Suggestions on Promoting the Development of Cruise Industry in China* was issued jointly by ten departments of the central government [1]. The document highlighted the great potential of China's cruise tourism industry and explicitly set the target of building one of the most dynamic markets in the cruise ship industry across the world by 2035. Yang [2] studied the cruise ship market in China, concluding that the development of the luxury cruise ship industry is of great importance to the economy. At present, China's economic development is in a transition period from high-speed growth to high-quality development. The shipbuilding industry should seize this opportunity to improve the industrial chain of designing and manufacturing high value-added ships, of which luxury cruise ships are important components. Vigorously developing China's do-

Received: 2021 − 01 − 21 **Accepted**: 2021 − 03 − 03

Supported by: National Natural Science Foundation of China (51879159, 51809169); Chang Jiang Scholars Program (T2014099); National Key R & D Program of China (2019YFB1704200, 2019YFC0312400); Ministry of Industry and Information Technology High Technology Ship Research Program; Zhejiang Provincial Natural Science Foundation (LY19A020001)

Authors: ZHANG Mu, male, born in 1997, master degree. Research interest: computational marine hydrodynamics. E-mail: M. Zhang@sjtu.edu.cn

WANG Jianhua, male, born in 1988, Ph.D. , associate professor. Research interests: computational marine hydrodynamics, ship maneuvering in waves. E-mail: jianhuawang@sjtu.edu.cn

WAN Decheng, born in 1967, Ph.D., professor, doctoral supervisor. Research interests: computational marine hydrodynamics, high performance computing, CFD and CAE software development. E-mail: dcwan@sjtu.edu.cn

***Corresponding author**: WAN Decheng

mestic cruise ship industry and studying luxury cruise ships become essential as the development of an "internal circular economy" is prioritized.

According to the literature survey, numerous studies have been conducted on the industrial development pattern, ship appearance, operating routes, and general hull arrangement of luxury cruise ships, whereas the hydrodynamic performance of cruise ships is rarely investigated. Cao et al [3] predicted the navigation performance of luxury cruise ships in light of the potential flow theory. Nevertheless, the results based on potential flow lacked details on the flow field. Wang et al [4] investigated the effect of stern flaps on the resistance on the cruise ship experimentally. Wang et al [5] optimized the bulbous bow line of a luxury cruise ship by a parametric approach. Liu et al [6] optimized the ship type in light of the potential flow theory with the aim of reducing the wave-making resistance on luxury cruise ships. Computational fluid dynamics-based (CFD-based) numerical simulation can provide some guidance for cruise ship design with the simulation of flow field details. The hydrodynamic solver naoe-FOAM-SJTU we developed can technically meet the precision requirements of hydrodynamic performance prediction of luxury cruise ships. Shen et al [7] used this solver to simulate the 10°/10° zigzag maneuvering of a KRISO container ship (KCS, a standard 3 600 TEU container ship type) and obtained sound calculation results. Liu et al [8] applied the naoe-FOAM-SJTU solver to simulate a Duisburg test case ship (DTC ship, a standard 14 000 TEU container ship type) under an oblique wave condition and summarized the rolling and pitching motions of the ship. The results obtained were in good agreement with the experimental results.

Due to its high accuracy in simulating maneuverability and seakeeping performance, the naoe-FOAM-SJTU solver was employed to predict the seakeeping performance of a luxury cruise ship under design under different wave heights (0.062 5, 0.1, 0.15, 0.225 m; the scale ratio of the model: 1∶40) and different wave directions with the same wave height (head sea, oblique wave, and beam sea with a wave height of 0.15 m). The predicted results were analyzed. This study is expected to provide reference data for safety and comfort evaluation of cruise ships and thereby offer theoretical guidance for cruise ship design.

1 Mathematical model

1) Reynolds-averaged Navier-Stokes (RANS) equation.

To solve unsteady incompressible viscous fluids, the solver adopts the incompressible two-phase RANS equation as the governing equation:

$$\nabla \cdot \boldsymbol{U} = 0 \tag{1}$$

$$\frac{\partial \rho \boldsymbol{U}}{\partial t} + \nabla \cdot (\rho(\boldsymbol{U} - \boldsymbol{U}_g)\boldsymbol{U}) = -\nabla p_d - \boldsymbol{g} \cdot x \nabla \rho + \nabla \cdot (\mu_{eff} \nabla \boldsymbol{U}) + (\nabla \boldsymbol{U}) \cdot \nabla \mu_{eff} + f_\sigma + f_s \tag{2}$$

where $\boldsymbol{U}$ is the velocity field; $\boldsymbol{U}_g$ is the grid moving velocity; $p_d = p - p\boldsymbol{g} \cdot x$, is the fluid hydrodynamic pressure, where p is the total pressure and $p\boldsymbol{g} \cdot x$ is the hydrostatic pressure; ρ is the density of the liquid or gas; $\boldsymbol{g}$ is the gravitational acceleration vector; x is the spatial coordinate; $\mu_{eff} = \rho(v + v_t)$, is the effective dynamic viscosity, where v and v_t are the kinematic viscosity and turbulent eddy viscosity, respectively, and the latter can be obtained by solving the turbulence model; f_σ is the surface tension term; f_s is the source term imposed on the wave absorbing region; t is the time.

2) Turbulence model.

Several turbulence models are available in OpenFOAM, although only two of them are currently prevalent: 1) the k-ω model proposed by Wilcox; 2) the SST k-ω model proposed by Menter that involves both calculating the interior of the boundary layer and simulating the turbulent region. Therefore, the SST k-ω model is adopted for hydrodynamic prediction of a luxury cruise ship in this study. The details about this model are omitted here as they can be found in Reference [9].

2 Overview of luxury cruise ship type and numerical prediction of seakeeping performance

2.1 Overview of ship type calculated

A certain type of luxury cruise ship was adopted as the research object of this study, and the main dimensions of the model-scale luxury cruise ship were summarized in Table 1. It should be noted that the calculation model adopted is a simplified one without superstructure since this study focuses on the hydrodynamic performance of the cruise ship and does not involve its wind resistance performance. Fig. 1 shows a model of the luxury cruise ship.

Table 1 Main dimensions of model−scale luxury cruise ship (scale factor: 40)

Parameter	Value
Length between perpendiculars L_{pp}/m	7.458 0
Molded breadth B/m	0.966 0
Molded depth D/m	0.684 0
Designed draft T/m	0.214 0
Block coefficient C_b	0.738 7

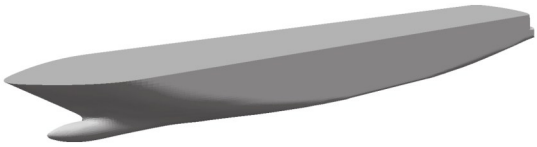

Fig. 1 Luxury cruise ship model

2.2 Evaluation criteria for seakeeping performance and parameter initialization for different working conditions

During their navigation in waves, cruise ships demonstrate significant motion responses, including rolling, pitching, and heaving occur, all of which compromise the comfort of the cruise ship. When the vertical acceleration of the ship exceeds 1/10 of the gravitational acceleration (0.1***g***), the seasickness of passengers on board aggravates, resulting in an unpleasant cruising experience and an indirect loss of the economic value added. In this study, the safety and comfort of the cruise ship were evaluated by comparing the simulation results with the corresponding criteria for ship safety and comfort. Table 2 shows the criteria for evaluating the seakeeping performance of ships. The values in the table are the root mean square (*RMS*).

Table 2 Evaluation criteria for ship seakeeping performance (*RMS*)

Criterion	Vertical acceleration ***g***	Rolling/(°)	Pitching/(°)	Reference
Safety standard	0.20	4.0	2.0	ISO 2631/3 1987&1982
Comfort standard	0.10	3.0	1.5	
Structural design standard	0.33	–	–	

Overlapping grids were adopted for griding in this study, and the details about this method can be found in Reference [10]. Fig. 2 shows the computational domain used for seakeeping performance calculation. The maximal dimensions along the length, width, and vertical directions of the ship were set to $8L_{pp}$, $3L_{pp}$, and $3L_{pp}$, respectively. The overlapping grid technique requires a set of hull grids and a set of background grids. Fig. 3 presents the overlapping grid layout, in which the number of hull grids is 1.63 million while that of background grids is 1.04 million.

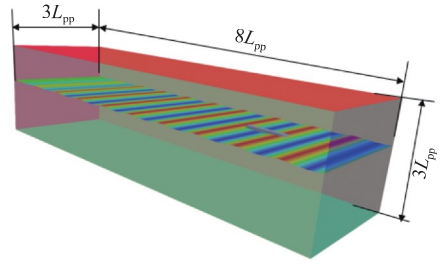

Fig. 2 Seakeeping performance calculation domain

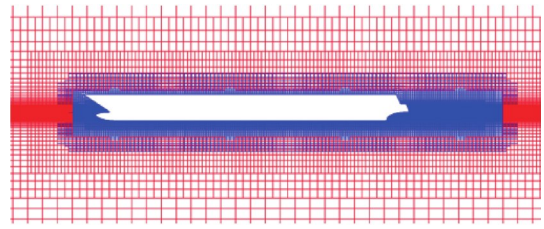

Fig. 3 Overlapping grids for seakeeping performance calculation

The wave calculated in this paper was regular. The maximal wave-induced disturbing force was obtained when the ship length/wavelength ratio L/λ was close to 1. To explore the large motion response of the cruise ship in regular waves, this paper set the wavelength λ to $1L_{pp}$. The parameter initialization for different working conditions is shown in Table 3.

Table 3 Parameter initialization for different working conditions

Working condition No.	Wave height/m	Wave direction angle/(°)	Wavelength λ	Period/s	*Fr*	Full-scale ship speed /kn
1	0.062 5	0				
2	0.1	0				
3	0.15	0	$1L_{pp}$	2.186	0.209 (maximum speed)	22
4	0.15	45				
5	0.15	90				
6	0.225	0	$1L_{pp}$	2.186	0.171 (design speed)	18

2.3 Numerical simulation of seakeeping performance under different wave heights

The following section presents a numerical simulation of the seakeeping performance of the cruise ship at the maximum speed under the head wave condition with different wave heights. Fig. 4 shows the time-history curves of the resistance on the model-

scale cruise ship and those of its motion responses when Fr = 0.209 and wave heights are 0.062 5, 0.1, and 0.15 m, respectively. According to Fig. 4(a), the resistance on the ship fluctuates increasingly violently as wave height rises. The minimum resistance falls to below zero when the bow is at the trough, leading to a negative resistance. Fig. 4(b) and Fig. 4(c) show that the heaving and pitching motions of the cruise ship fluctuate in a pulsatile manner over time, i.e., the values of the motions exhibit the characteristics of sinusoidal curves, and the average amplitudes of the motions increase with wave height. The *RMS* values of pitching motion are 0.660, 0.984, and 1.394 when wave heights are 0.062 5, 0.1, and 0.15 m, respectively, which meet the standards of ship comfort as specified in the evaluation criteria for ship seakeeping performance. Fig. 4(d) indicates that the rolling motions under different wave heights are beyond distinct patterns, and the changes in their amplitude with an increasing wave height are irregular as well.

The time-history curves presented in this paper are the vertical accelerations at the center of gravity. Those at the bow and stern are derived according to the acceleration correlation between two points in a rigid body. Fig. 4(e) shows that the amplitude of the vertical acceleration increases more obviously under a larger wave height. Specifically, the *RMS* values of vertical accelerations at the bow, midship, and stern are 0.994, 0.766, and 0.917, respectively, under a wave height of 0.15 m (corresponding to a full-scale wave height of 6 m). Therefore, they satisfy the comfort requirement that the *RMS* of the vertical acceleration should not exceed 0.1***g*** specified in the evaluation criteria for ship seakeeping performance listed in Table 2. The designed cruise ship thus meets the comfort requirements in head waves.

2.4 Numerical simulation of seakeeping performance under different wave directions

The cruise ship resistance, acceleration, and motion at three wave angles of head waves, beam waves, and oblique waves were compared under the maximum speed and a wave height of 0.15 m (corresponding to a full-scale wave height of 6 m). The results show that the highest and lowest average amplitudes of resistance were obtained under oblique wave and beam waves conditions, respectively. The time-history curves of resistance are shown in Fig. 5.

According to Fig. 5(b), the average amplitude of the heaving motion does not change much as the wave direction angle increases. Nevertheless, the period of the heaving motion under the beam wave

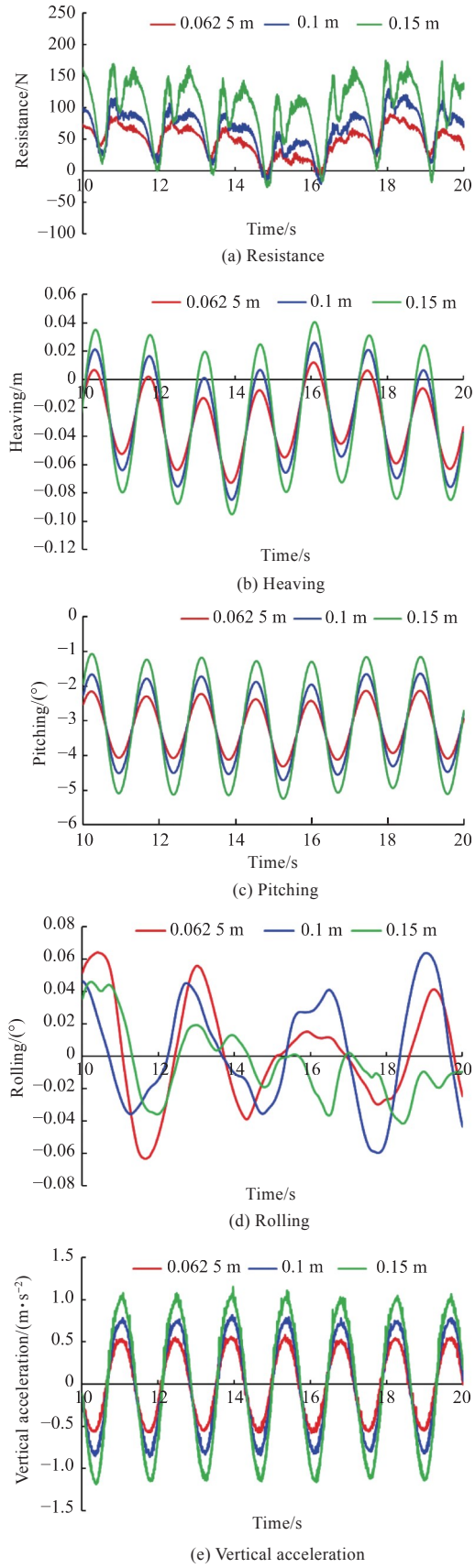

Fig. 4 Time-history curves of resistance and motion response under different wave heights

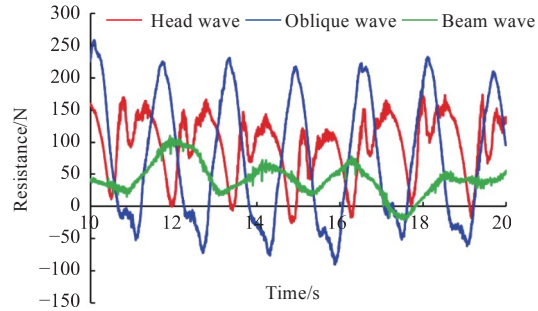

(a) Resistance

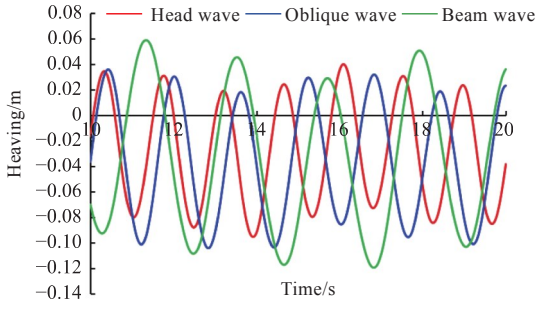

(b) Heaving

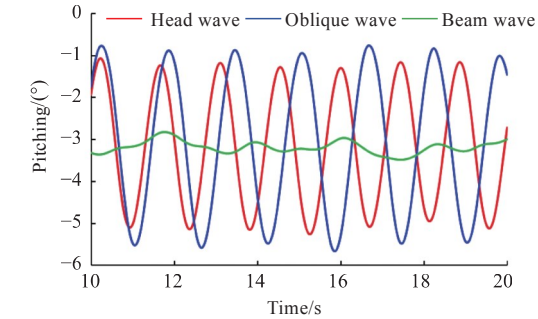

(c) Pitching

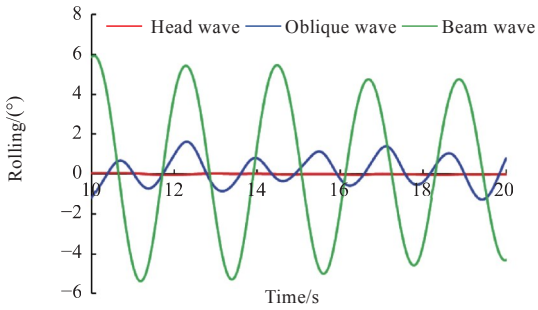

(d) Rolling

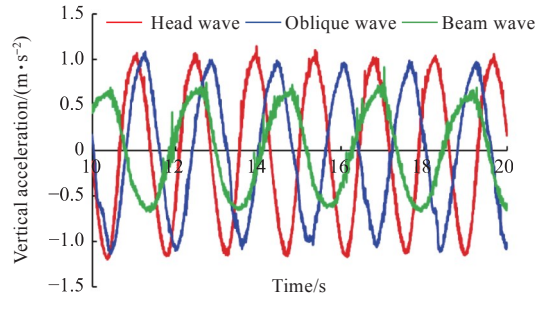

(e) Vertical acceleration

Fig. 5 Time-history curves of resistance and motion response under a wave height of 0.15 m

condition is significantly different from those under the oblique wave and head wave conditions, and the phases obtained under the latter two wave directions are also significantly different.

As can be seen from Fig. 5(c), the pitching motion has the smallest amplitude under the beam wave condition and the largest amplitude in the oblique wave. The *RMS* value of the pitching motion in the oblique wave is 1.67, which meets the safety standard in the ISO specification.

Fig. 5(d) suggests that the rolling motion has the largest amplitude under the beam wave condition, with an *RMS* value of 3.76. This value still meets the safety requirements in the evaluation criteria for ship seakeeping performance issued by the Health and Safety Committee of the International Organization for Standardization (ISO).

According to Fig. 5(e), the *RMS* values of vertical acceleration at the bow, midship, and stern under a wave height of 0.15 m are 0.994, 0.766, and 0.917, respectively, given the *RMS* values of vertical acceleration in the head wave condition calibrated in Fig. 4(e) in Section 2.3. Under the oblique wave condition, the *RMS* values of vertical acceleration at the bow, midship, and stern are 0.845, 0.685, and 0.923, respectively. Moreover, the *RMS* values at the bow, amidships, and stern are 0.703, 0.462, and 0.697, respectively, under the beam wave condition. The *RMS* values obtained under the three wave directions all match the comfort criteria in the specification.

2.5 Analysis of green water on deck under large wave heights

Massive green water on deck was observed under the working condition of a wave height of 0.225 m (corresponding to a full-scale wave height of 9 m) and the designed speed. The green water on deck simulated during CFD-based prediction is shown in Fig. 6. Generally, the process can be divided into 4 stages: 1) Waves break into the bow; 2) the bow starts to rise; 3) the bow starts to fall; 4) Waves break into the bow again.

This paper focuses on the resistance, heaving, pitching, and vertical acceleration under a wave height of 0.225 m and the designed speed (Fr= 0.171). As can be seen from the time-history curves in Fig. 7, the resistance under this condition undergoes violent oscillation, and the variation period is also significantly different from that under a small wave height. At the model scale, the maximum amplitude of the heaving motion reaches 0.1 m when the designed draft is 0.214 m. The *RMS* value of the pitching motion is 1.937° and thus meets the re-

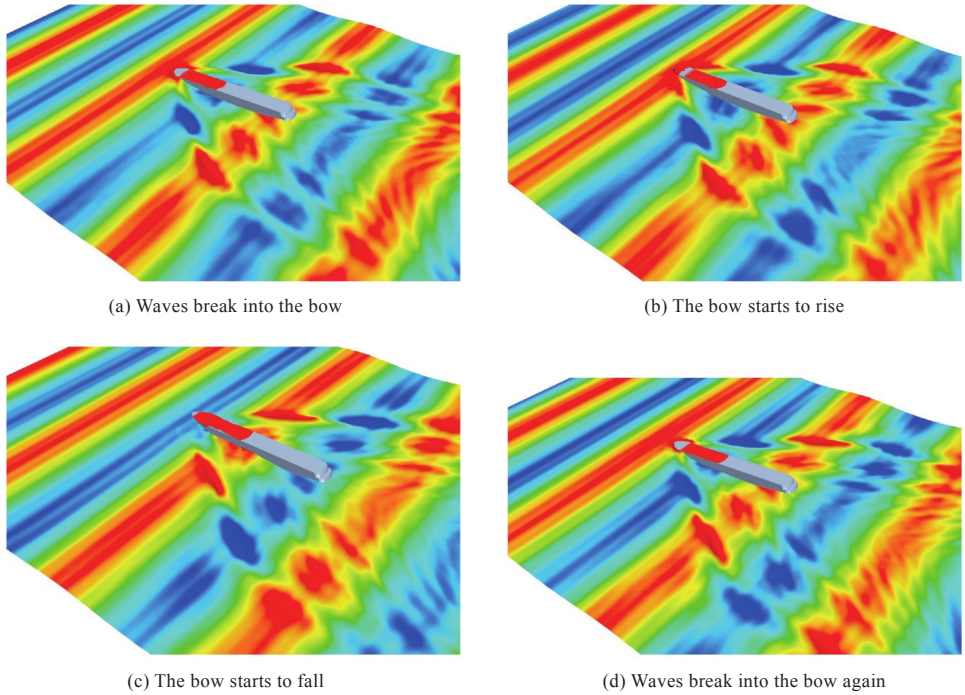

(a) Waves break into the bow (b) The bow starts to rise

(c) The bow starts to fall (d) Waves break into the bow again

Fig. 6 Time-history curves of resistance and motion response under a wave height of 0.225 m

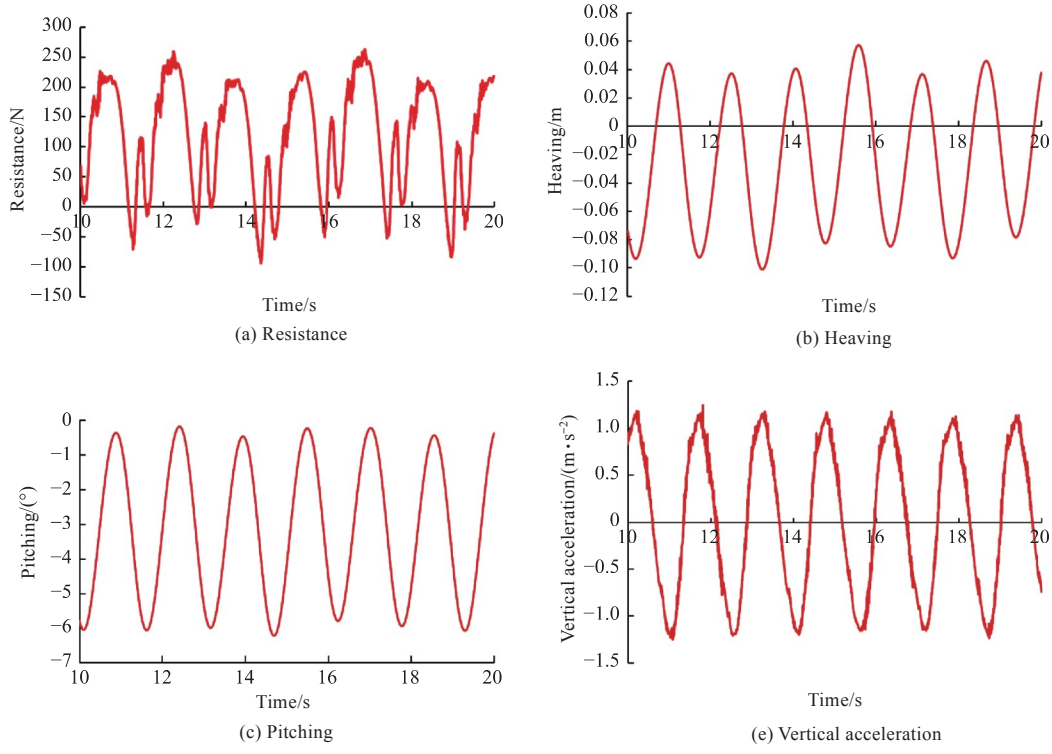

(a) Resistance (b) Heaving

(c) Pitching (e) Vertical acceleration

Fig. 7 Time-history curves of resistance and motion response under a wave height of 0.225 m and Fr=0.171

quirements of the safety standard. The *RMS* values of vertical acceleration at the bow, midship, and stern are 1.637, 0.798, and 1.264, respectively, and they also meet the requirements of the safety standards.

The model-scale cruise ship calculated in this paper is a simplified model without superstructure, which may affect the precision of the calculation results. Therefore, superstructure-included models can be adopted in future research for modification.

3 Conclusions

In this study, a numerical simulation of the seakeeping performance of a luxury cruise ship under design was conducted with an overlapping grid technique embedded in a self-developed hydrodynamic solver naoe-FOAM-SJTU on the basis of the RANS equation. The main conclusions obtained are

as follows.

1) When navigating at the maximum speed under a head wave condition with wave heights of 0.062 5, 0.1, and 0.15 m, respectively, the cruise ship is subject to a periodic resistance, and the average amplitudes of its pitching and heaving motions increase with wave height. Under these three conditions, the cruise ship's vertical acceleration, rolling, and pitching all meet the comfort requirements specified by ISO.

2) When the cruise ship navigates at the maximum speed under a wave height of 0.15 m, all its motion indicators meet the ship comfort standard under the head wave and beam wave conditions. In contrast, all its motion indicators except the *RMS* value of its pitching motion meet the comfort criteria under the oblique wave condition, although the latter still meets the safety criteria.

3) The cruise ship demonstrates the most violent motion response when it navigates at the designed speed under the head wave condition with the maximum wave height (0.225 m). Although green water on deck was observed, its motion responses still meet the safety criteria.

The numerical simulation results of the cruise ship's seakeeping performance in this study can be used to guide and corroborate model tests of cruise ships in an efficient manner. Our future work will further investigate the motion of model-scale superstructure-included cruise ships in irregular waves.

References

[1] FENG L, YUAN B.Some opinions and suggestions on promoting the development of cruise industry in China [EB/OL]. (2018-09-29) [2019-06-20]. http://finance.people. com. cn/n1/2018/0927/c1004-30317446. html (in Chinese).

[2] YANG T Y. Analysis on the development path of Shanghai luxury cruise ship supporting industry [J]. Shanghai University of Engineering Science, 2018 (36): 29−31.

[3] CAO Y, YU B J, WANG J F. Modeling the seakeeping performance of luxury cruise ships [J]. Journal of Marine Science and Application, 2010, 9 (3): 292−300.

[4] WANG Y X, PENG B Y, ZHAO Q. Experimental study on the influence of trim flap on the resistance of a medium-sized luxury cruise [J]. Chinese Journal of Hydrodynamics (Ser. A), 2017,32 (6):725−731 (in Chinese).

[5] WANG S, WANG Y X, ZHAO Q, et al. Bulbous bow optimization for a medium-sized luxury cruise based on parametric design method [J]. Journal of Jiangsu University of Science and Technology (Natural Science Edition), 2017, 31 (5): 646−649 (in Chinese).

[6] LIU X W, WAN D C. Hull form optimization of wavemaking resistance in different speeds for a luxury cruise ship [J]. Chinese Journal of Ship Research, 2020, 15 (5): 1−10, 40 (in Chinese).

[7] SHEN Z R, WAN D C, CARRICA P M. Dynamic overset grids in OpenFOAM with application to KCSself-propulsion and maneuvering [J]. Ocean Engineering, 2015, 108: 287−306.

[8] LIU C, WANG J H, WAN D C. CFD computation of wave forces and motions of DTC ship in oblique waves [J]. International journal of offshore and polar engineering, 2018, 28 (2): 154−163.

[9] MENTER F R. Two-equation eddy-viscosity turbulence models for engineering applications [J]. AIAA Journal, 1994, 32 (8): 1598−1605.

[10] SHEN Z R. Development of overset grid technique for hull-propeller-rudder interactions [D]. Shanghai: Shanghai Jiao Tong University, 2014 (in Chinese).

基于重叠网格的豪华邮轮多工况耐波性数值分析

张牧[1,2], 王建华[1,2], 万德成*[1,2]

1 上海交通大学 船海计算水动力学研究中心,上海 200240

2 上海交通大学 船舶海洋与建筑工程学院,上海 200240

摘　要:[**目的**]在豪华邮轮的设计阶段,为了节约成本,需采用流体动力学(CFD)方法对设计中的邮轮进行耐波性能预报。[**方法**]以一艘大型豪华邮轮为研究对象,使用自主开发的船舶水动力学CFD求解器naoe-FOAM-SJTU对模型尺度下的豪华邮轮进行耐波性数值模拟。耐波性的模拟在造波方式上采用速度入口输入式造波,对不同波高和不同浪向下的邮轮运动进行预报和总结。[**结果**]评估发现,目前设计得到的邮轮船模在最大航速、波高为0.062 5, 0.1和0.15 m工况下基本符合船舶舒适性要求;在设计航速下、波高为0.225 m、迎浪工况下符合船舶安全性要求。[**结论**]在完成计算的工况下,邮轮的船型设计符合船舶耐波性评估标准中的安全标准和舒适性标准。

关键词:豪华邮轮;重叠网格;耐波性评估;naoe-FOAM-SJTU